

# Heat of Adsorption of Carbon Monoxide on a Pd/Rh Three-Way Catalyst and on a Rh/Al<sub>2</sub>O<sub>3</sub> Solid

Olivier Dulaurent,\* Karine Chandes,† Christophe Bouly,† and Daniel Bianchi\*<sup>1</sup>

\*Laboratoire d'Application de la Chimie à l'Environnement (LACE), UMR 5634, Université Claude Bernard, Lyon-I, Bat. 308, 43 Boulevard du 11 Novembre 1918, 69622 Villeurbanne, France; and †ECIA-Equipement et Composants pour l'Industrie Automobile, BP 17, Bois sur prés 25550 Bavans, France

Received June 10, 1999; revised February 11, 2000; accepted February 14, 2000

In previous studies it has been shown that the change of the FTIR spectra of the adsorbed CO species formed on supported metal (Pt and Pd) catalysts with the adsorption temperature  $T_a$  (range 300–800 K) can lead to the determination of the heat of adsorption of each adsorbed CO species (linear CO species on Pt-containing solids, and linear and bridged CO species on Pd-containing solids). In the present study, this procedure is used for the determination of the heats of adsorption of the two adsorbed CO species formed on Pd sites in the presence of a second metal to form a Pd/Rh three-way catalyst. In a first step the heats of adsorption of CO on a reduced 3% Rh/Al<sub>2</sub>O<sub>3</sub> solid are determined. On this solid, the adsorption of CO leads to the formation of linear and bridged CO species on Rh sites. It is shown that the heats of adsorption of the two species vary with the coverage according to linear relationships: from 195 kJ/mol at  $\theta = 0$  to 103 kJ/mol at  $\theta = 1$  for the linear CO species and from 125 kJ/mol at  $\theta = 0$  to 75 kJ/mol at  $\theta = 1$  for the bridged CO species. On palladium-containing solids with and without Rh, the adsorption of CO at  $T > 300$  K leads to IR bands attributed mainly to linear and bridged CO species on Pd sites. It is shown that the heat of adsorption of the linear CO species (varying from 54 kJ/mol at  $\theta = 1$  to 92 kJ/mol at  $\theta = 0$ ) is not modified by the presence of Rh. For the bridged CO species, the heat of adsorption is slightly decreased, at high coverages, in the presence of Rh but is not modified at low coverages (i.e., at  $\theta = 0.95$  the heats of adsorption of the bridged CO species are 113 and 100 kJ/mol on the monometallic and the bimetallic solids respectively whereas at  $\theta = 0.52$  the heat of adsorption is 135 kJ/mol on the two solids). © 2000 Academic Press

**Key Words:** carbon monoxide; palladium; rhodium; three-way catalyst; FTIR; heat of adsorption; adsorption model.

## I. INTRODUCTION

The determination of the heats of adsorption of the various adsorbed CO species (linear, bridged, multibound) on supported metal catalysts is one of the important methods of characterization of the CO surface interaction. For a given CO partial pressure  $P_a$  and at an adsorption temperature  $T_a$ , this parameter controls the coverage of these

<sup>1</sup>To whom correspondence should be addressed. E-mail: daniel.bianchi@univ-lyon1.fr.

adsorbed CO species. In previous works, it has been shown that the evolution of the FTIR spectra of the adsorbed CO species, formed on Pt- (1) and Pd- (2, 3) containing solids, during the adsorption of CO at various temperatures  $T_a$ , can lead to the determination of the coverage of each species (i.e., linear and bridged CO species) as a function of  $T_a$ . Using an adsorption model, the curves provide the heat of adsorption of each adsorbed CO species as a function of the coverage. This method is experimentally easy and has been used to study the effects on the heats of adsorption of various parameters involved in the preparation of the catalyst, such as (a) the nature of the support (1, 3), (b) the nature of the salt used as a precursor of the metallic phase (with and without chlorine) (3), and (c) the presence of a second metal in bimetallic particles Pt/Rh (1). The comparison with the literature data has shown that there is a good agreement with the heats of adsorption determined on monocrystals and model particles as well as on supported metal catalysts using microcalorimetric methods (1–3 and references therein). The present study concerns the heat of adsorption of CO on a Pd/Rh three-way catalyst. The main objective is the determination of a possible influence of Rh on the heat of adsorption of CO on the Pd sites (2, 3). The heats of adsorption of the linear and bridged CO species on a reduced Rh/Al<sub>2</sub>O<sub>3</sub> solid are also determined and compared with those observed on the Pd/Rh solid. The results presented in this study lead us to reconsider slightly our conclusions on a Pt/Rh catalyst (1).

## II. EXPERIMENTAL

### (a) Catalysts

**Pd/Rh three-way catalyst.** The composition of the solid was 1.3% Pd/0.2% Rh/11% La<sub>2</sub>O<sub>3</sub>/37% CeO<sub>2</sub>/Al<sub>2</sub>O<sub>3</sub> (in wt%). The La<sub>2</sub>O<sub>3</sub>/CeO<sub>2</sub>/Al<sub>2</sub>O<sub>3</sub> support was prepared according to the following procedure. Alumina ( $\gamma$ -Al<sub>2</sub>O<sub>3</sub>, from Condea) was impregnated with an aqueous solution of cerium acetate. The solvent was evaporated slowly and the powder was dried for 12 h at room temperature and

then for 4 h at 393 K before treatment in air for 2 h at 773 K. After this treatment the powder was impregnated with an aqueous solution of lanthanum acetate. After the drying procedure as described above the solid was treated in air for 2 h at 773 K. The noble metals Pd and Rh were deposited on the support (in a single step) using a solution containing  $\text{H}_2\text{PdCl}_4$  (obtained from acid dissolution of  $\text{PdCl}_2$ ) and  $\text{RhCl}_3$ . After the drying procedure the powder was treated in air at 773 K for 2 h.

**Rh/Al<sub>2</sub>O<sub>3</sub> solids.** A 0.6% Rh/Al<sub>2</sub>O<sub>3</sub> (in wt%) solid was prepared according to the following procedure:  $\gamma$ -alumina from Condea was introduced slowly in an aqueous solution of  $\text{RhCl}_3$ . After 24 h of agitation at room temperature, the suspension was slowly heated to evaporate the solvent. The powder was treated in air for 4 h at 393 K followed by 2 h at 773 K. A 3% Rh/Al<sub>2</sub>O<sub>3</sub> solid was prepared according to the following procedure:  $\gamma$ -alumina from Degussa was impregnated (by the incipient wetness method) with an aqueous solution of  $\text{RhCl}_3$ . After drying for 12 h at room temperature and 24 h at 373 K, the solid was treated for 3 h in air at 773 K (heating rate 2 K/min).

Some results are described on a monometallic solid: 1.96% Pd/16% La<sub>2</sub>O<sub>3</sub>/56% CeO<sub>2</sub>/Al<sub>2</sub>O<sub>3</sub> prepared as above with an  $\text{H}_2\text{PdCl}_4$  solution (2).

For the determination of the efficiency of the bimetallic solid as a three-way catalyst, it has been deposited on a cylindrical cordierite monolith structure ( $\Phi = 2.5$  cm,  $L = 5.5$  cm) to obtain a precious metal loading of around 4 g/l and a Pd/Rh weight ratio of 6.5, values which were similar to those found for commercial monoliths for vehicle.

For the FTIR study of the adsorbed species the powders were compressed to form a disk ( $\Phi = 1.8$  cm) which was placed in the sample holder of the IR cell described briefly below. Before the adsorption of CO (using a 1% CO/He mixture), the solids were treated *in situ* (150 cm<sup>3</sup>/min) according to the following procedure: oxygen ( $T = 713$  K,  $t = 30$  min)  $\rightarrow$  helium ( $T = 713$  K,  $t = 30$  min)  $\rightarrow$  hydrogen ( $T = 713$  K,  $t = 1$  h)  $\rightarrow$  hydrogen (adsorption temperature)  $\rightarrow$  helium (10 min)  $\rightarrow$  1% CO/He.

#### (b) Efficiency of the Pd/Rh Solid as a Three-Way Catalyst

The performances of the solids as a three-way catalyst were determined by an analytical system described elsewhere (4, 5). Synthetic gas mixtures (CO/NO/propene/propane/O<sub>2</sub>/CO<sub>2</sub>/H<sub>2</sub>O/N<sub>2</sub>) of compositions similar to that of automobile exhaust gas were used to determine, with hourly space velocities similar to real conditions (75,000–100,000 h<sup>-1</sup>), the efficiency of catalysts deposited on a monolith structure ( $\Phi = 2.5$  cm,  $L = 5.5$  cm). The performances were characterized by studying the conversion of the pollutants as a function either of the inlet gas temperature (light-off) or of  $\lambda$ , the air–fuel equivalence ratio (without and with perturbation of the value of  $\lambda$ ). The compo-

sition of the gas at the outlet of the stainless steel reactor, to determine the conversions of the reactive gas (CO, NO<sub>x</sub>, hydrocarbon), was determined by FTIR spectroscopy.

#### (c) IR Cell in Transmission Mode To Study the Adsorbed Species at High Temperatures

The FTIR spectra (Nicolet Protege FTIR spectrometer, resolution 4 cm<sup>-1</sup>) of the adsorbed CO species (transmission mode) on the prepared solids, in the presence of the CO/He mixture, were recorded by using a small internal volume stainless steel IR cell described elsewhere (1). The disks of solid (weight range 40–100 mg) were placed between two CaF<sub>2</sub> windows 2.2 mm apart. This small volume increased the ratio between the incoming signal due to the adsorbed species and that due to the gas-phase species. This cell allowed *in situ* treatments of the solids, at atmospheric pressure, with a gas flow rate in the range 150–2000 cm<sup>3</sup>/min, and at temperatures in the range 293–900 K.

### III. RESULTS AND DISCUSSION

The main objective of the present work is to study the modifications of the heat of adsorption of each adsorbed CO species (linear and bridged species) formed on the palladium atoms by the introduction of rhodium to produce a three-way catalyst. However, in a first step we present the efficiency of the prepared bimetallic solids as a three-way catalyst.

#### (a) Efficiency of the Pd/Rh-Containing Solid as a Three-Way Catalyst

Figure 1 gives the conversions of CO, NO, and HC (HC means both propene and propane) at 723 K, as a function of  $\lambda$ , the air/fuel equivalence ratio on the Pd/Rh/La<sub>2</sub>O<sub>3</sub>/CeO<sub>2</sub>/Al<sub>2</sub>O<sub>3</sub> catalyst. As expected (5, 6) for a three-way catalyst, the prepared solid permits a high

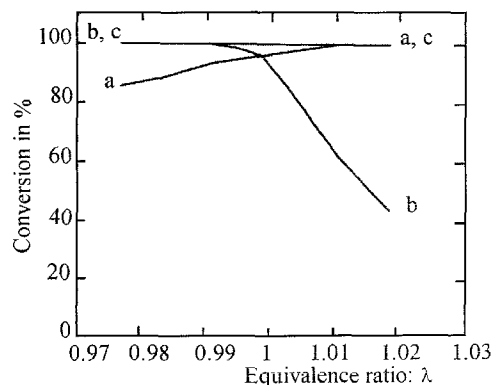


FIG. 1. Efficiency of the Pd/Rh/La<sub>2</sub>O<sub>3</sub>/CeO<sub>2</sub>/Al<sub>2</sub>O<sub>3</sub> three-way catalyst as a function of the air/fuel equivalence ratio: conversion of CO (a), NO (b), and hydrocarbon (c).

conversion of the three pollutants at  $\lambda = 1$ . The conversion of NO decreases at  $\lambda > 1$  (excess of  $O_2$ ) and the CO conversion decreases at  $\lambda < 1$ . The conversion of the HC is high whatever the  $\lambda$  values while on a prepared Pt/Rh three-way catalyst the conversion of the HC followed that of CO (1). These curves are similar to those obtained with commercial monolith catalysts (5–7). This result confirms that the prepared Pd/Rh solid is representative of a commercial three-way catalyst.

(b) FTIR Spectra during the Adsorption of 1% CO/He at Various Temperatures on the Pd/Rh Solid

Figure 2 compares the FTIR spectra recorded at 300 K after adsorption of a 1% CO/He mixture on the Pd/La<sub>2</sub>O<sub>3</sub>/CeO<sub>2</sub>/Al<sub>2</sub>O<sub>3</sub> solid (spectrum a) and on the Pd/Rh three-way catalyst (spectrum b). The two solids lead to the appearance of two main IR bands above and below 2000 cm<sup>-1</sup> indicating the formation of linear (denoted L) and bridged (denoted B) CO species respectively (2 and references therein). The IR bands of the L species are situated at 2087 and 2090 cm<sup>-1</sup> for the Pd/Rh- and the Pd-containing solid respectively, whereas the B species gives the same IR band at 1965 cm<sup>-1</sup> on the two solids. Figure 2 shows that there are very few modifications of the FTIR spectra due to the presence of the rhodium. However, a weak shoulder can be observed around 2050 cm<sup>-1</sup> in spectrum b. In the following part of this study, it is shown that this shoulder is due to the adsorption of CO on the rhodium sites of the Pd/Rh particles. Figure 3 shows the evolution of the IR bands with  $T_a$  on the bimetallic solid. For the IR band of the B species a slight increase of the IR band between 300 and 430 K is observed without any shift. For higher temperatures a shift is recorded to lower wavenumbers (1962 cm<sup>-1</sup> at 460 K, 1957 cm<sup>-1</sup> at 508 K, 1931 cm<sup>-1</sup> at 608 K, and

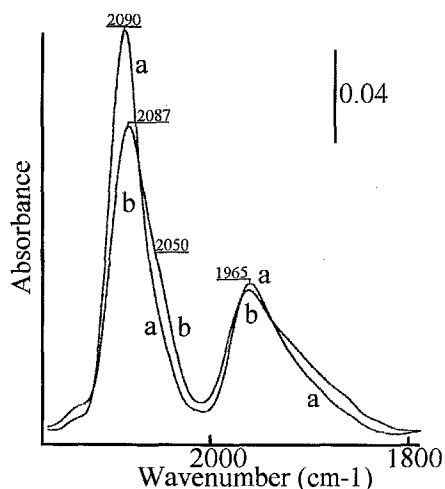


FIG. 2. FTIR spectra recorded at 300 K on the reduced solids: (a) Pd monometallic solid and (b) Pd/Rh three-way catalyst.

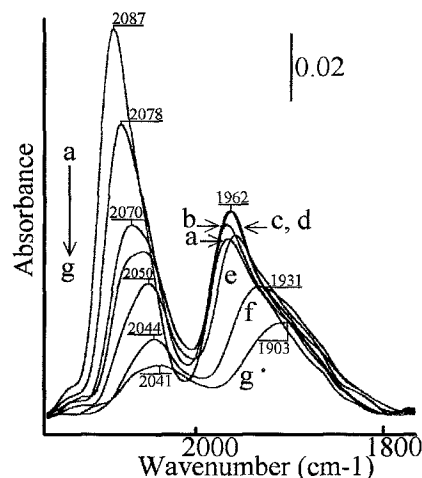


FIG. 3. Infrared spectra taken during the adsorption of CO (1% CO/He) on the Pd/Rh three-way catalyst: (a) 300 K, (b) 329 K, (c) 430 K, (d) 460 K, (e) 508 K, (f) 608 K, and (g) 686 K.

1903 cm<sup>-1</sup> at 686 K) associated with a progressive decrease in intensity of the IR band. The intensity of the IR band of the L species is constant between 300 and 310 K and then decreases progressively associated with a shift to lower wavenumbers (2087 cm<sup>-1</sup> at 300 K, 2078 cm<sup>-1</sup> at 365 K, and 2070 cm<sup>-1</sup> at 430 K). For  $T_a > 430$  K, the decrease in intensity of the main IR band leads to better detection of the shoulder at 2050 cm<sup>-1</sup> which is finally detected as a distinct IR band. This band shifts to 2044 cm<sup>-1</sup> at 608 K. At the highest temperature used (683 K) a broad IR band is detected at 2041 cm<sup>-1</sup>. Note that on various monometallic Pd-containing solids (3) we have shown that there are probably two linear CO species having different heats of adsorption. The IR band of the first adsorbed species, denoted L<sub>1</sub>, with the lowest heat of adsorption (varying from 92 kJ/mol at  $\theta = 0$  to 54 kJ/mol at  $\theta = 1$ ), dominated the spectra at low adsorption temperatures. The IR band of the second species, denoted L<sub>2</sub> (with a heat of adsorption >165 kJ/mol) was detected only at high temperatures when the coverage of the L<sub>1</sub> species was low. However, on Pd-containing solids, the IR bands of the L<sub>1</sub> and L<sub>2</sub> species were strongly overlapped and rarely discernible (2, 3). This means that the detection of two IR bands above 2000 cm<sup>-1</sup> in Fig. 3, in the range 430–608 K, indicates (a) that the adsorbed CO species on the Pd/Rh surface are different from those on the surface of the Pd monometallic solids, and (b) that probably the rhodium atoms are involved in the CO adsorption in addition to L<sub>2</sub> species on Pd sites. Thus, before the determination of the heat of adsorption of the adsorbed species on the Pd/Rh solid, we present in the following section the FTIR spectra taken during the adsorption of CO at various temperatures on two Rh/Al<sub>2</sub>O<sub>3</sub> solids. These data are used for the determination of the heats of adsorption of the linear and bridged CO species on rhodium sites.

The following notations are used to identify the various adsorbed species: (a)  $L_1/Pd$ ,  $L_2/Pd$ , and  $B/Pd$  indicate the two linear and the bridged CO species on the palladium sites of the monometallic solid respectively; (b)  $L/Rh$  and  $B/Rh$  indicate the linear and bridged CO species on the rhodium sites of the monometallic solid; (c)  $L_i/Pd(-Rh)$  ( $i = 1$  or  $2$ ) and  $B/Pd(-Rh)$  indicate the linear and bridged CO species on the palladium sites of the bimetallic particles; (d)  $L/Rh(-Pd)$  and  $B/Rh(-Pd)$  are the linear and bridged CO species on the rhodium sites of the bimetallic particles; and (e)  $B/(Pd-Rh)$  is the bridged CO species on the sites involving Pd and Rh on the bimetallic particles.

(c) *FTIR Spectra during the Adsorption of CO at Various Temperatures on Rh/Al<sub>2</sub>O<sub>3</sub>*

The adsorption of CO at 300 K on a reduced Rh-containing solid with a metal loading similar to that of the bimetallic solid (0.6% Rh/Al<sub>2</sub>O<sub>3</sub>) leads to spectrum a in Fig. 4. Two IR bands are observed at 2092 and 2021 cm<sup>-1</sup> (with the first one slightly more intense than the second one) indicating the formation of *gem*-dicarbonyl CO species in agreement with the literature data on Rh/Al<sub>2</sub>O<sub>3</sub> catalysts with similar metal loadings (8–10 and references therein). The absence of these two IR bands after the adsorption of CO on the reduced bimetallic solid (Fig. 2) is interpreted considering that the rhodium fraction of the three-way catalyst is not present as monometallic particles but forms bimetallic particles with Pd. This interpretation has been previously suggested to explain the absence of *gem*-dicarbonyl species on a Pt/Rh solid (1, 11). Note that some authors have observed *gem*-dicarbonyl species on Pt/Rh catalysts (9, 12) and this indicates that the preparation methods as well as the pretreatments of

the catalysts may affect the distribution of Rh on the surface of the bimetallic catalysts. The modifications (not shown) of the spectra during the interaction of CO at high temperatures on the 0.6% Rh/Al<sub>2</sub>O<sub>3</sub> are complex and very different from those observed on the Pd/Rh solid. These data cannot be used to interpret the observations on the Pd/Rh catalyst. However, the increase in the rhodium loading (3% Rh/Al<sub>2</sub>O<sub>3</sub>) leads to FTIR spectra after adsorption of CO which permit us (a) to explain the change of the FTIR spectra recorded at high temperatures on the Pd/Rh solid, and (b) to determine the heat of adsorption of the various adsorbed species.

Spectrum b in Fig. 4 recorded at 300 K after adsorption of 1% CO/He on the fresh reduced 3% Rh/Al<sub>2</sub>O<sub>3</sub> solid indicates a strong IR band at 2065 cm<sup>-1</sup> due to a linear CO species (13–15 and references therein) associated with a shoulder at 2020 cm<sup>-1</sup> corresponding to one of the two IR bands of the *gem*-dicarbonyl species (the second IR band at  $\approx 2090$  cm<sup>-1</sup> is overlapped with the strong IR band of the linear CO species). A broad IR band is detected at 1861 cm<sup>-1</sup> with a shoulder at 1900 cm<sup>-1</sup> which indicates that more than one bridged CO species (15, 16) are formed after the adsorption of CO at 300 K. Spectrum c is recorded at 300 K on the 3% Rh/Al<sub>2</sub>O<sub>3</sub> solid which has been treated at 713 K with the 1% CO/He mixture followed by a reduction of the solid at 713 K. The aging of the solid during the CO adsorption at high temperatures leads to the almost disappearance of the *gem*-dicarbonyl species and to a decrease in the intensities of the linear and bridged CO species. After this first aging, two consecutive adsorptions of CO at high temperatures do not lead to significant differences in the intensities of the IR bands after adsorption of CO at 300 K. The absence of the IR bands of the *gem*-dicarbonyl species and the intensities of the two IR bands of the  $L/Rh$  and  $B/Rh$  species (spectrum c in Fig. 4) allow us to study the evolution of the coverages of the L and B species on the Rh sites with  $T_a$  and thus to determine the heats of adsorption of the two species at various coverages. It must be noted that the intensity of the IR band of the B species at 300 K is just enough to achieve the study. Figure 5 shows the spectra recorded on the aged and reduced 3% Rh/Al<sub>2</sub>O<sub>3</sub> solid during the adsorption of 1% CO/He at various temperatures. From 300 to 453 K the IR band area of the L species increases slightly and is associated with a progressive shift from 2065 to 2055 cm<sup>-1</sup>. After cooling down of the sample from 453 to 350 K, it is observed that the intensity of the IR band is constant. This indicates that the modifications of the IR band during the heating is irreversible and may indicate a reconstruction of the CO/Rh system in the presence of CO. For  $T_a > 520$  K, the IR band shifts to lower wavenumbers (2046 cm<sup>-1</sup> at 543 K, 2042 cm<sup>-1</sup> at 653 K, 2037 cm<sup>-1</sup> at 673 K, 2030 cm<sup>-1</sup> at 696 K, and 2023 cm<sup>-1</sup> at 723 K) and its intensity decreases progressively. The intensities of the two IR bands of the bridged species decrease also after 450 K

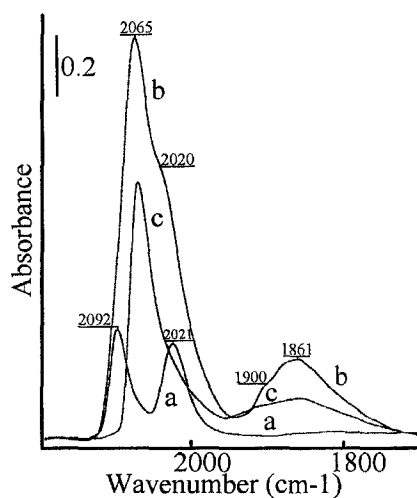


FIG. 4. FTIR spectra recorded at 300 K on the reduced solids: (a) 0.6% Rh/Al<sub>2</sub>O<sub>3</sub>, (b) 3% Rh/Al<sub>2</sub>O<sub>3</sub> (fresh catalyst), and (c) 3% Rh/Al<sub>2</sub>O<sub>3</sub> (used catalyst).

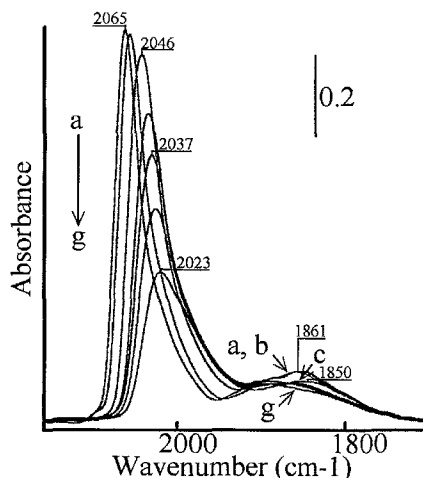


FIG. 5. Infrared spectra taken during the adsorption of CO (1% CO/He) on 3% Rh/Al<sub>2</sub>O<sub>3</sub>: (a) 300 K, (b) 383 K, (c) 543 K, (d) 653 K, (e) 673 K, (f) 696 K, and (g) 723 K.

and shift to lower wavenumbers (the positions of the main IR band are 1861 cm<sup>-1</sup> at 300 K and 1850 cm<sup>-1</sup> at 543 K, and the positions of the shoulder are 1911 cm<sup>-1</sup> at 300 K and 1896 cm<sup>-1</sup> at 618 K). For  $T_a > 618$  K, the two IR bands of the bridged CO species are strongly overlapped, leading to the detection of a broad IR band with a maximum at 1859 cm<sup>-1</sup>.

(d) *Heats of Adsorption of the Linear and of the Bridged CO Species on 3% Rh/Al<sub>2</sub>O<sub>3</sub>*

The spectra in Fig. 5 can be used for the determination of the evolution of the coverage of L/Rh and B/Rh species with  $T_a$  as described in previous studies with Pt- (1) and Pd- (2, 3) containing solids. The coverage,  $\theta$ , of an adsorbed species at  $T_a$  is obtained using the IR band area of its characteristic IR band,  $\theta = (\text{the IR band area at } T_a / \text{the highest IR band area})$ . This determination of  $\theta$  assumes (a) a linear relationship between the intensity of the IR band and the amount of adsorbed CO species on the surface and (b) that the IR absorption extinction coefficients are independent of  $T_a$  as studied by Rasband and Hecker (17) on various Rh/SiO<sub>2</sub> catalysts. There is a controversy over the above assumption (a). In particular, on monocrystals the linear relationship between the IR band area and the coverage is mainly observed for  $\theta < \approx 0.8$  while for  $\theta > 0.8$  the IR band area roughly tends to a constant value. However, on a Pd/SiO<sub>2</sub> catalyst Hicks *et al.* (18) have observed that the curve (integrated absorbance for the IR bands of adsorbed CO species) =  $f$  (amount of CO on the surface) was a straight line until the saturation of the surface. Using the analytical method of Refs. (17, 18), Srinivas and Chuang (19) have observed on Rh/SiO<sub>2</sub> catalysts that the IR absorption coefficients ( $\bar{A}_{CO}$ ) for the linear and bridged CO species were approximately constant as a function of different parameters (the error in calculating

$\bar{A}_{CO}$  was  $\approx 20\%$ ) and they used these values for the determination of the amount of each adsorbed species under hydroformylation reaction at 513 K. In a recent study (20), we proved the validity of assumption (a) for the linear CO species adsorbed on a Pt/Al<sub>2</sub>O<sub>3</sub> catalyst. In particular, for  $T_a > 520$  K, we have determined the same values for the coverage of the linear CO species ( $\theta$  range 1–0.6) using either FTIR measurements (with the above assumptions) or a carbon mass balance with a mass spectrometer (20). Moreover, the decrease in intensity of the IR band with  $T_a$  may also be due to a decrease in the number of metallic sites adsorbing the species by poisoning. For instance, the dissociation/disproportionation reaction of CO at high temperatures may lead to C deposition and/or O adsorption on the metallic surface. This is evaluated by comparing, in Fig. 6, the FTIR spectra recorded at 300 K before (spectrum a) and after (spectrum b) heating in 1% CO/He at 713 K followed by cooling to room temperature in the presence of CO. A significant decrease (by  $\approx 40\%$ ) in the IR band area for the L species is observed due to the poisoning of the sites. The intensity of the IR band of the bridged CO species is not strongly modified after adsorption at 713 K. If  $T_a < 653$  K, the intensity of the IR band of the L/Rh species is not modified after cooling down of the sample in CO, indicating that C and/or O deposition leads to a modification of the surface only for  $T_a > 653$  K.

Curve a in Fig. 7 shows the evolution of the coverage of the L/Rh species with  $T_a$  using the results in Fig. 5. From 300 to  $\approx 450$  K the increase corresponds to the reconstruction of the CO/surface system as described above. At  $\approx 640$  K there is a breaking point due to the decrease in the number of sites by poisoning of the surface (Fig. 6). However, if for the highest adsorption temperature ( $T_a = 713$  K) we use as highest IR band area that of spectrum b in Fig. 6, the

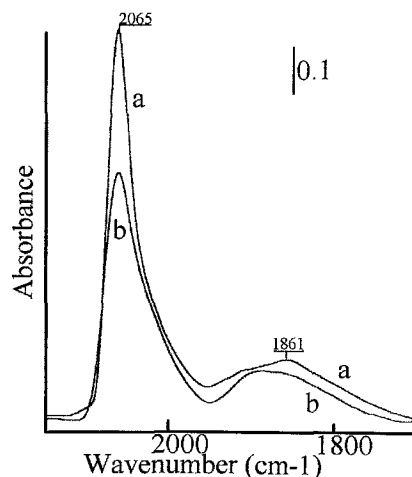


FIG. 6. Infrared spectra after adsorption of CO (1% CO/He) at 300 K on 3% Rh/Al<sub>2</sub>O<sub>3</sub>: (a) on the reduced solid and (b) after heating at 723 K and cool down to 300 K in 1% CO/He.

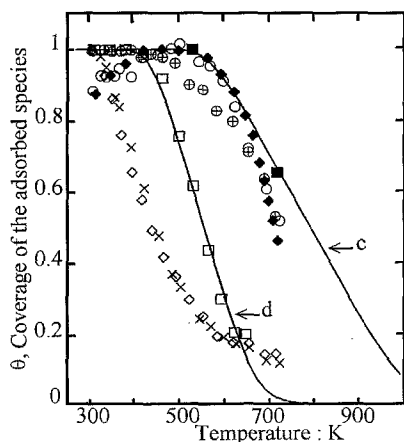


FIG. 7. Evolution of the coverages of the linear and bridged CO species with the adsorption temperature:  $\blacklozenge$ , (a) and  $\square$ , (b) experimental data on 3% Rh/Al<sub>2</sub>O<sub>3</sub> for the linear and bridged CO species, respectively;  $\blacksquare$ , experimental coverage of the linear CO species on 3% Rh/Al<sub>2</sub>O<sub>3</sub>, after correction (see the text); (c) and (d) coverage of the linear and bridged CO species on 3% Rh/Al<sub>2</sub>O<sub>3</sub> according to expressions [1] and [2];  $\times$ , (e) and  $\circ$ , (f) experimental data on the Pd monometallic solid for the linear and bridged CO species respectively;  $\diamond$ , (g) and  $\oplus$ , (h) experimental data on the Pd/Rh three-way catalyst linear and bridged CO species, respectively.

coverage of the sites is given by the symbol  $\blacksquare$  in Fig. 7 (another value of the coverage is reported after cooling down of the sample to 570 K, second  $\blacksquare$  symbol). The experimental data of curve a in Fig. 7 for  $T_a < 640$  K and the corrected coverage at 713 K (symbol  $\blacksquare$ ) lead to a profile  $\theta = f(T_a)$  very similar to those observed previously for the adsorbed CO species on Pt- (1) and Pd- (2, 3) containing solids. This profile indicates a linear increase in the heat of adsorption with a decrease in coverage.

Assuming a linear relationship between the heat of adsorption and the coverage  $\theta$  of the sites,  $\theta$  is given by ((1, 2) and references therein)

$$\theta = \frac{RT_a}{\Delta E} \ln \left( \frac{1 + \lambda_0 P_a}{1 + \lambda_1 P_a} \right), \quad [1]$$

where  $\Delta E$  is the difference in the heats of adsorption of the adsorbed species at  $\theta = 0$  ( $E_0$ ) and  $\theta = 1$  ( $E_1$ ),  $P_a$  and  $T_a$  are the partial pressure of CO and the adsorption temperature respectively, and  $\lambda_0$  and  $\lambda_1$  are the adsorption coefficients at  $\theta = 0$  and  $\theta = 1$  given by the statistical thermodynamics assuming the loss of three degrees of translation ((1) and references therein),

$$\lambda = \frac{h^3}{k(2\pi mk)^{3/2}} \frac{1}{T_a^{5/2}} \exp \left( \frac{E_d - E_a}{RT_a} \right) \quad [2]$$

where  $h$  is Planck's constant,  $k$  is Boltzmann's constant,  $m$  is the weight of the CO molecule,  $E_d$  and  $E_a$  are the activation energies of desorption and adsorption respectively,

while  $E_d - E_a$  is the heat of adsorption at a given coverage. To determine the heats of adsorption at  $\theta = 0$  and  $\theta = 1$ , it is only required to find the  $E_1$  and  $E_0$  values which lead to a theoretical curve  $\theta = f(T)$  (expressions [1] and [2]) in accord with the experimental data (curve a). Curve c in Fig. 7 is obtained using in expressions [1] and [2]  $E_0 = 195$  kJ/mol at  $\theta = 0$  and  $E_1 = 103$  kJ/mol at  $\theta = 1$ . It can be observed that there is a good agreement between the experimental data for the linear CO species (curve a for  $T_a < 640$  K and the corrected coverage at 713 K) and the adsorption model. The accuracy on the value of the coverage is  $\theta \pm 0.02$  and that on the heat of adsorption is  $E_i \pm 5$  kJ/mol. Curve b in Fig. 7 shows the evolution of the coverage of the B/Rh species with  $T_a$  in the temperature range 300–650 K. For  $T_a > 650$  K there is an uncertainty on the determination of the IR band area due to its weak intensity. The profile of curve b is also in agreement with an adsorption model assuming a linear decrease in the heat of adsorption with the increasing coverage. Curve d is obtained using  $E_0 = 125$  kJ/mol and  $E_1 = 75$  kJ/mol in expression [1] and [2]. The above values for the heats of adsorption of the linear and bridged CO species can be compared with those found in the literature on Rh single-crystal surface.

Dubois and Somorjai (21) and Dubois *et al.* (22) used energy loss spectroscopy (ELS) to characterize the adsorbed species formed on Rh(111) (21) and on stepped single-crystal Rh(331) (22). On Rh(111), at low exposures of CO ( $< 0.4$  L, 1 L = 1 Langmuir =  $10^{-6}$  Torr s<sup>-1</sup>), the authors observe an energy loss at 1990 cm<sup>-1</sup> ascribed to a linear CO species. For higher exposure, a second energy loss is detected at 1870 cm<sup>-1</sup> that is attributed to bridged CO species whereas the energy loss of the linear CO species shifts to higher wavenumbers. The intensities of the two species increase with the exposure (increase in coverage) and for a pressure of  $10^{-5}$  Torr, two well-defined peaks are detected at 1870 and 2070 cm<sup>-1</sup>. The comparison of these data with the LEED pattern led the authors to suggest a structure for the adsorption of CO on the Rh(111) surface indicating that the linear/bridged species ratio is 2. On Rh(311) at 0.1 L a single energy loss is recorded at 2060 cm<sup>-1</sup> and at 0.2 L a second energy loss is detected at 1930 cm<sup>-1</sup> (22). The intensities of the two peaks increase in the range 0.2–1 L and are constant in the range 1–20 L. However, in contrast to the Rh(111), the positions of the IR bands stay constant in the range 0.1–20 L. The 2060 cm<sup>-1</sup> peak is ascribed to linear CO species on a single atom of Rh(111) terraces while the 1930 cm<sup>-1</sup> peak is attributed to bridged CO species located along the step edges or at least to the step atoms. On model Rh particles (2–3 nm diameter) deposited on Al<sub>2</sub>O<sub>3</sub>, ELS studies indicate (23) two peaks at 1870 and 2020 cm<sup>-1</sup> whatever the exposure (highest value  $10^{-5}$  Torr) which are assigned to bridged and linear CO species respectively. Delouise *et al.* (24) have studied using XPS and LEED the surface composition of the adsorbed species formed on

Rh(111) and Rh(331) after adsorption of CO and they compared their results to those found using ELS (22). In agreement with ELS results the authors observe the formation of two species on the Rh surface: a CO atop species and a bridged CO species corresponding to the species leading to stretching frequency at 1980 and 1840  $\text{cm}^{-1}$  respectively (21, 22). The authors (24) compare the proportion of the two adsorbed species as a function of the backpressure and of the coverage of the surface. On Rh(111), they observe that the bridged/atop ratio increases from 0 at low coverage to 0.72 at high coverages. This is because the atop species is formed first at low coverage while the bridged CO species appears progressively with increases in coverage. Note that in a recent study Beutler *et al.* (25) using the same analytic methods on Rh(111) recorded the two above adsorbed species but with another ratio. The above studies show that there is a good agreement between the observations on single crystals and on supported metal catalysts (if one excepts the detection of *gem*-dicarbonyl species on highly dispersed rhodium catalysts): at high coverages all the solids lead to the formation of linear and bridged CO species. This justifies the validity of a comparison between the heat of adsorption of the adsorbed CO species on the Rh monocrystals and on the Rh-supported catalyst. It must be noted that the linear as well as the bridged CO species are not identical on the various solids: at a given coverage, the position of their respective IR bands depends on the solid. This must be taken into account for the comparison of the heats of adsorption of the various adsorbed species.

On Rh(111), Dubois and Somorjai (21) have shown that the bridged CO species can be selectively removed by slowly heating the sample in a vacuum at 360 K while the coverage of the linear CO species is only slightly affected. The same observations were noted in (24). This indicates that the heat of adsorption of the bridged CO species is significantly lower than that of the linear CO species and this conclusion agrees with the values determined in the present study; i.e., at low coverage of the sites, the heats of adsorption are 195 and 125 kJ/mol for the linear and the bridged CO species respectively.

The heats of adsorption of the adsorbed CO species on Rh single crystals are mainly determined by TPD methods considering a nondissociative chemisorption and using either a preexponential factor of  $10^{13} \text{ s}^{-1}$  for the rate constant of desorption or without any assumption on this parameter using the method of Chang *et al.* (26). The TPD spectra recorded on various monocrystals, Rh(111) (27–29), Rh(331) (30), Rh(100) (27), Rh(311) (31), and Rh(110) (32, 33), indicate a single peak at short exposure (<1 L) corresponding to the linear CO species (21). At long exposure (1–100 L), (a) the intensity of this first peak increases alongside a shift to lower temperatures (decrease in the heat of adsorption with increase in coverage), and (b) a new peak

is detected at low temperatures corresponding to bridged CO species (21). It must be noted that if two overlapped TPD peaks are detected after adsorption of CO at  $L > 1$ , the literature data report only a single heat of adsorption corresponding to the linear CO species. Assuming a preexponential factor of  $10^{13} \text{ s}^{-1}$ , Castner *et al.* (27) found that the heat of adsorption of CO is 130 kJ/mol on Rh(111) and 122 kJ/mol on Rh(100) at an exposure of 5 L corresponding to the linear CO species. This exposure leads to a significant coverage of the surface not indicated in (27) but which can be estimated to be  $\theta \approx 0.5$  assuming  $\theta \approx 1$  at 1000 L (see Fig. 8b of Ref. 27). Note that Thiel *et al.* (28) found a coverage of 0.87 at 3.8 L on Rh(111) with a slight contribution of the bridged CO species. In our case the heat of adsorption of the linear CO species is given by  $E = (195 - 92 \theta)$  kJ/mol, leading to 149 kJ/mol at  $\theta = 0.5$  in reasonable agreement with the value quoted in (27) (the value is 114 kJ/mol assuming  $\theta = 0.87$ ). However, Batteas *et al.* (31) report the heats of adsorption of CO on various Rh monocrystals, (311), (110), (100), and (111), and conclude that this parameter is structure insensitive at low coverage  $\approx 130$  kJ/mol (structure sensitive at high coverage). On Rh(111), Thiel *et al.* (28) found a value of  $132 \pm 8$  kJ/mol in the limit of zero coverage with a preexponential factor of  $10^{13.6} \text{ s}^{-1}$  and observe a decreasing linear relationship with the coverage  $E_d = (132 - 226 \theta)$  kJ/mol in the range  $\theta < 0.25$ . Belton and Schmiege (29) using the method of Chang *et al.* (26) found 132 kJ/mol with a preexponential factor of  $1.3 \cdot 10^{13} \text{ s}^{-1}$  on Rh(111) at  $\theta = 0.03$ . The authors (29) found a similar value for the heat of adsorption of the linear CO species on Rh model particles deposited on  $\text{Al}_2\text{O}_3$  (size 2 and 7 nm) and conclude that at low coverage the heat of adsorption is independent of the particle sizes. Assuming a preexponential factor of  $10^{13} \text{ s}^{-1}$ , they found a heat of adsorption of 125 kJ/mol at  $\theta = 1$ . This last value is in agreement with that found in the present study (103 kJ/mol). More recently, Nehasil *et al.* (34) report a heat of adsorption of CO of 137 kJ/mol on Rh foils and 120 kJ/mol on Rh model particles on  $\text{Al}_2\text{O}_3$  (size = 2.5 nm) in the limit of zero coverage. The heats of adsorption decrease with an increase in coverage according to linear relationships and at  $\theta = 1$  the values are 127 and 110 kJ/mol for the Rh foil and the 2.5 nm Rh particles respectively (34). An attempt to achieve a deconvolution of the recorded TPD peaks on Rh(111) assuming two species of different activation energies of desorption is described by Belton *et al.* (29). They have found that the activation energies of the two species must be  $(141 - 2\theta)$  kJ/mol (linear CO species) and  $(125 - 4\theta)$  kJ/mol (bridged CO species). Note that the last value at low coverage is in agreement with that determined in the present study for the B/Rh species. Campbell and White (35) using TPD found, at various coverages, a heat of adsorption of 134 kJ/mol on an Rh film with a preexponential factor of  $10^{13} \text{ s}^{-1}$ . The aforementioned values for the heat of adsorption of the CO species leading to the

TPD peak at high temperatures (L/Rh species) are mainly in a range 130–140 kJ/mol in the limit of the 0 coverage. These values are significantly lower than that found in the present study, 195 kJ/mol. Note that in early works, reported by Somorjai (36), values of  $\approx 190$  kJ/mol were determined on Rh film, in particular using a calorimetric method (37). Moreover, Baraldi *et al.* (33) in a comparative study of the adsorption of CO on (1 × 1) and (1 × 2) Rh(110) (38) have shown, using TPD analysis (Chang *et al.* method (26)), that there are significant differences in the heats of adsorption of CO on the two surfaces. At around  $\theta = 0.2$ , the heats of adsorption are 145 and 100 kJ/mol on the (1 × 1) and (1 × 2) surfaces respectively (33) with a preexponential factor of  $\approx 10^{13}$  s<sup>-1</sup>. For the two surfaces they observe a decreasing linear relationship with the coverage leading to 50 and 15 kJ/mol at  $\theta = 1$  on (1 × 1) and (1 × 2) surfaces respectively with a preexponential factor of  $10^4$  s<sup>-1</sup>. The extrapolation of the heats of adsorption at the limit of  $\theta = 0$  gives 130 kJ/mol for the (1 × 2) surface (in agreement with the values found in the literature) and 180 kJ/mol for the (1 × 1) surface. This last value is in agreement with the heat of adsorption of the L/Rh species found in the present study (195 kJ/mol). Note that if at high coverages the preexponential is assumed to be  $10^{13}$  s<sup>-1</sup>, the heat of adsorption in (33) changes from 70 kJ/mol to around 105 kJ/mol on the (1 × 1) surface. This last value is in agreement with our data (103 kJ/mol) for the L/Rh species.

Finally, it appears that the heat of adsorption of the L/Rh species at low coverage determined in the present study (195 kJ/mol) is significantly higher than those found on several oriented planes ( $\approx 130$ – $140$  kJ/mol) but is in agreement with that found more recently on (1 × 1) Rh(110) surface (33). We have not found in the literature (except in Ref. (29)) any data on the heat of adsorption of the bridged CO species in order to establish a comparison with our values. This last remark shows that one of the advantages of the present procedure, compared with the TPD method, for the determination of the heat of adsorption of the individual adsorbed CO species (linear and bridged), is the absence of a complex deconvolution of the recorded data.

*Remarks.* On Rh(210), after a high exposure of CO at 300 K, Rebholz *et al.* (39) observe three peaks at 376, 425, and 452 K on the TPD spectra, attributed respectively to  $\alpha_1$ ,  $\alpha_2$ , and  $\alpha_3$  species. The  $\alpha_1$  species which is detected only at saturation of the surface differentiates the observations of the aforementioned studies on the various Rh single crystals. The point of interest is that the authors note that only the  $\alpha_3$  species (usually ascribed to linear CO species) is involved in the CO dissociation at high temperatures. This is in agreement with our observations in Fig. 6 which indicate that it is the IR band of the linear CO species which is significantly affected ( $-40\%$ ) after adsorption of CO at high temperatures.

(e) *Heat of Adsorption of the Adsorbed CO Species on the Pd/Rh Three-Way Catalyst*

Curves e and f in Fig. 7 give the evolution of the coverage of the L/Pd (L means that the L<sub>1</sub>/Pd and L<sub>2</sub>/Pd species are not distinguished) and B/Pd species on the monometallic solid, Pd/La<sub>2</sub>O<sub>3</sub>/CeO<sub>2</sub>/Al<sub>2</sub>O<sub>3</sub>, according to a procedure described elsewhere (2, 3). We have shown that curve e overlaps those obtained on various Pd-containing solids, in particular Pd/Al<sub>2</sub>O<sub>3</sub>. (2). This was used to conclude that the values of the coverage (at given  $T_a$  and  $P_a$ ) and of the heat of adsorption of the linear CO species (at a given  $\theta$ ) are not significantly modified by several parameters such as the nature of the support (Al<sub>2</sub>O<sub>3</sub>, CeO<sub>2</sub>/Al<sub>2</sub>O<sub>3</sub>, La<sub>2</sub>O<sub>3</sub>/CeO<sub>2</sub>/Al<sub>2</sub>O<sub>3</sub>) or the salt precursor of the metallic phase (with and without chlorine). Curve e is due to the presence of two linear CO species (2, 3): an L<sub>1</sub>/Pd species which dominates the FTIR spectra at low temperatures (with a heat of adsorption varying linearly with the coverage from  $E_0 = 92$  kJ/mol at  $\theta = 0$  to  $E_1 = 54$  kJ/mol at  $\theta = 1$ ) and an L<sub>2</sub>/Pd species (with a heat of adsorption  $>165$  kJ/mol) present in lower amount than the L<sub>1</sub> species which dominated the FTIR spectra at high temperatures. Similarly curve f indicates (2, 3) the presence of a B/Pd species with a heat of adsorption which linearly decreases with increase in coverage from  $E_0 = 168$  kJ/mol at  $\theta = 0$  to  $E_1 = 105$  kJ/mol at  $\theta = 1$ . For the B/Pd species,  $E_0$  was independent of the nature of the support and of the salt precursor of the metallic phase while  $E_1$  was significantly modified by the above parameters. For instance, on a Pd/Al<sub>2</sub>O<sub>3</sub> solid prepared with PdCl<sub>2</sub> we determined  $E_1 = 75$  kJ/mol. It can be observed that the heat of adsorption of the L/Rh species (195 kJ/mol at  $\theta = 0$  and 103 kJ/mol at  $\theta = 1$ ) is (a) higher than that of the L<sub>1</sub>/Pd whatever the coverage, and (b) similar to that of the L<sub>2</sub>/Pd species. This indicates that, if the L<sub>1</sub>/Pd and L/Rh species are present on the Pd/Rh three-way catalyst, the increase in  $T_a$  must affect the L<sub>1</sub>/Pd species first and then the L/Rh species (while the L<sub>2</sub>/Pd species can be present with the L/Rh species). The reverse is true for the B species: the coverage of the B/Rh species must decrease at a lower adsorption temperature (low heat of adsorption) than that of the B/Pd species. The above remarks permit us to interpret the evolution of the spectra recorded in the course of CO adsorption at high temperatures on the Pd/Rh solid (Fig. 3).

The molar Pd/Rh ratio is 6.2, assuming (a) a similar surface composition of the bimetallic particles, and (b) similar absorption coefficients for the IR bands of the L<sub>1</sub>/Pd–(Rh) and L/Rh–(Pd) species, it must be concluded that the spectra recorded at low adsorption temperatures (high coverage of both linear CO species) are dominated by the IR band of the L<sub>1</sub>/Pd–(Rh) species. The IR band of the L/Rh–(Pd) species is strongly overlapped with that of the L<sub>1</sub>/Pd–(Rh) species and leads to a weak shoulder at 2050 cm<sup>-1</sup> in Fig. 2b. Note that the Pd/Rh ratio at the



surface maybe is higher than 6.2, if it is considered that the surface is enriched in Pd as is the case on Pt/Rh solids (40). The increase in  $T_a$  leads to the decrease in the coverage of the  $L_1$ /Pd-(Rh) species having a lower heat of adsorption than the L/Rh-(Pd) species. For instance, curve e in Fig. 7 shows that at 450 K the coverage of the L/Pd species is  $\approx 0.45$  while that of the L/Rh species is 1 (curve a). This indicates that the contribution of the L/Rh-(Pd) species to the spectra recorded on the Pd/Rh solid increases with an increase in  $T_a$ . This explains that if at 300 K the L/Rh-(Pd) species is detected as a shoulder of the main IR band of the  $L_1$ /Pd-(Rh) species, then for  $T_a$  in the range 430–608 K, the contribution of the IR band of the L/Rh-(Pd) species increases and is clearly detected in Figs. 3d and 3e. However, as the heat of adsorption of the  $L_2$ /Pd species ( $> 165$  kJ/mol) is similar to that of the L/Rh species it can be assumed that the FTIR spectra e–f in Fig. 3 correspond to an overlap of the IR bands of the two species. Curve g in Fig. 7 gives the evolution of the coverage of the L species on the Pd/Rh solid without the differentiation of the  $L_1$ /Pd-(Rh) and L/Rh-(Pd) species (as in curve e for the  $L_1$ /Pd and  $L_2$ /Pd species of the Pd monometallic solid). The comparison of curves g and e shows that there are no significant differences between the two solids. This is because the IR band of the  $L_1$ /Pd species dominates the FTIR spectra on the two solids at low adsorption temperatures. We have not tried to achieve the deconvolution of the recorded IR bands of the linear species on Pd/Rh to reveal the accurate contribution of the  $L_1$ /Pd-(Rh) and of the L/Rh-(Pd) species because the exact profiles of the individual IR bands are not known. Moreover, the profile of the IR band of the  $L_2$ /Pd-(Rh) species is also not known with accuracy. However, the overlap of curves e and g clearly indicates that the heat of adsorption of the linear species on the palladium sites is not significantly modified by the presence of Rh in the bimetallic particles. It is not possible to propose the same conclusion for the L/Rh species due to the absence of deconvolution. However, the decrease in the IR band of the L/Rh-(Pd) species (for  $T_a > 508$  K, Fig. 3) is detected in the same range of temperatures as for the L/Rh species (Fig. 5), indicating that the heats of adsorption are not strongly affected by the presence of Pd. Note that we assume that the Rh fraction of the three-way catalyst forms bimetallic particles with the palladium fraction because in the case of the Rh monometallic solid with the same metal loading we have recorded the *gem*-dicarbonyl species.

Curve h in Fig. 7 shows that the coverage of the B species on the Pd/Rh solid (a single IR band is considered) decreases at a lower temperature than on the Pd monometallic solid (Fig. 7f). It seems that at high coverages of the Pd/Rh surface, the rhodium either decreases the heat of adsorption of the B/Pd species or is involved in the formation of B/(Pd-Rh) species. For  $T_a > 620$  K curves h and f in Fig. 7 are overlapped, indicating the same heat of adsorption of the bridged CO species on the two solids (Pd and Pd/Rh)

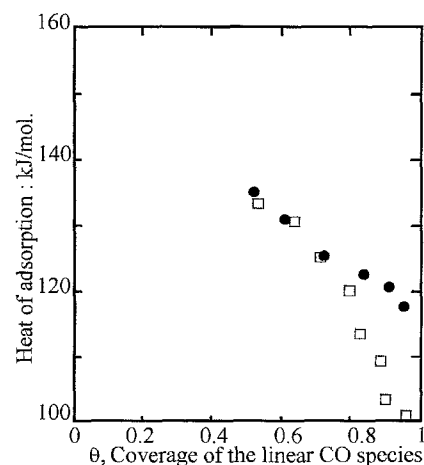


FIG. 8. Heat of adsorption of the bridged CO species at various coverages: ●, (a) Pd monometallic solid and □, (b) Pd/Rh three-way catalyst.

for coverage lower than 0.8. One of the consequences of the profile of curve h is that the heat of adsorption of the B species on the Pd/Rh solid does not follow a linear decreasing relationship with the coverage  $\theta$  in the full range of  $\theta$  in contrast to the Pd monometallic solids. The above remarks can be quantified as in (1), by the determination of the heat of adsorption of an adsorbed species at various coverage considering (a) Langmuir's model ( $\theta = LP_a/(1 + LP_a)$ ) for an adsorption without dissociation, (b) the adsorption coefficient,  $L$ , given by the statistical thermodynamics (expression [2]), and (c) that at each coverage is a corresponding value of the heat of adsorption. Figure 8 compares the evolution of the heat of adsorption of the bridged CO species on the Pd/Rh catalyst (curve b) and on the Pd monometallic solid (curve a) using the experimental coverages reported in Fig. 7 (curves f and h). It can be observed in Fig. 8 that (a) the heat of adsorption of the B species on the three-way catalyst is lower than that on the monometallic solid for  $\theta > 0.7$ , and (b) the same values are obtained for a coverage lower than 0.7. Note that the difference between the two heats of adsorption is not very strong. For instance, at  $\theta = 0.9$  the values are 105 and 120 kJ/mol on the bimetallic and monometallic solid respectively. This leads to the conclusion that if the rate of a given catalytic reaction involving CO on Pd catalysts is significantly modified (for instance factor of 5) by the presence of Rh, it is not the modifications of the heats of adsorption of CO which can be used as argument (there is not a factor of 5 between the coverages of the CO species on Pd and Pd/Rh solids). We have interpreted the profile of curve h in Fig. 7 for  $\theta > 0.8$  considering that the variation of the heat of adsorption of the B/Pd-(Rh) species with the coverage is not linear on the full range 0–1 (Fig. 8). However, it cannot be ruled out that it is the FTIR response which changes with the coverage (interactions between the various adsorbed molecules of the bimetallic catalyst) but it is difficult to experimentally

verify this explanation using a procedure similar to that described in (20).

(f) *Comments on the Adsorption of CO on Two Three-Way Catalysts: Pt/Rh and Pd/Rh*

One of the characteristics of the adsorption of CO on reduced three-way catalysts, either Pt/Rh (1) or Pd/Rh (present study), is the very low surface amount of *gem*-dicarbonyl species compared with the observations on a monometallic Rh solid with the same Rh loading. On solids with a high Rh loading the *gem*-dicarbonyl species are also very low (Figs. 5 and 6). These two observations lead to the conclusions that (a) to observe *gem*-dicarbonyl species the rhodium must be very dispersed (41), and (b) on the three-way catalysts the Rh is not very well dispersed because it is present in bimetallic particles. Note that another interpretation can be that in the presence of palladium, rhodium forms monometallic particles of large size and that the results observed on the Pd/Rh solids are only an overlap of the observations on Pd and Rh particles. However, this does not explain the values of the heat of adsorption of the bridged CO species at high coverage on the Pd/Rh solid (Fig. 8).

In a previous work (1) we have determined the heat of adsorption of the linear CO species formed on a Pt/Rh solid. A single IR band was observed above  $2000\text{ cm}^{-1}$  whatever  $T_a$ . We have discussed (1) the fact that it is difficult to determine if the Rh fraction of the Pt/Rh is involved in the IR band considering that the linear CO species give similar IR bands on Pt and Rh. Finally, considering (a) that a Rh monometallic solid with the same loading that the Pt/Rh catalyst only leads to *gem*-dicarbonyl species, and (b) that the surface of bimetallic particles Pt/Rh can be enriched in Pt (40), we have assumed that the IR band on the Pt/Rh solid was only due to Pt sites. The data described in the present study on the 3% Rh/Al<sub>2</sub>O<sub>3</sub> solid lead us to reconsider our previous conclusions. The evolutions of the coverage of the L/Rh species with  $T_a$  are very close to those observed on Pt monometallic solids and on the Pt/Rh three-way catalyst (1). This means that in (1) it was not possible to establish a distinction between the linear CO species formed on Pt and on Rh and that the IR band recorded on the Pt/Rh solid was probably the result of the overlapping of the IR bands of species formed on Pt (main contribution) and on Rh as observed in the present study. However, the main conclusion of (1) is in agreement with that of the present study: the heat of adsorption of the linear CO species either on Pt or on Pd is only slightly modified by the introduction of Rh as the second metal to form a three-way catalyst.

### CONCLUSION

The results of the present study on the evolution of the IR spectra of adsorbed CO species on Rh-containing solids

and on a Pd/Rh catalyst with the adsorption temperature  $T_a$  lead to the following conclusions.

On a reduced 3% Rh/Al<sub>2</sub>O<sub>3</sub> solid, the heat of adsorption of a linear CO species varies with the coverage according to a linear relationship from 195 kJ/mol at  $\theta = 0$  to 103 kJ/mol at  $\theta = 1$ . The heat of adsorption of a bridged CO species varies with the coverage according to a linear relationship from 125 kJ/mol at  $\theta = 1$  to 75 kJ/mol at  $\theta = 0$ .

On a 1.3% Pd/0.2% Rh/11% La<sub>2</sub>O<sub>3</sub>/37% CeO<sub>2</sub>/Al<sub>2</sub>O<sub>3</sub> three-way catalyst, two linear CO species are formed on Pd and Rh sites present in bimetallic particles. The IR band of the linear CO species on palladium atoms dominates the IR spectra at low temperatures. The linear CO species on Rh atoms is only well detected for  $T_a > 405\text{ K}$ . The heat of adsorption of the L species on palladium is not modified by the presence of Rh and varies with the coverage according to a linear decreasing relationship from  $E_0 = 92\text{ kJ/mol}$  at  $\theta = 0$  to  $E_1 = 54\text{ kJ/mol}$  at  $\theta = 1$  (2).

The heat of adsorption of the B species on the Pd/Rh solid is equal to that of the B/Pd species on monometallic solids for coverages lower than  $\theta = 0.8$ . For  $\theta > 0.8$ , the heat of adsorption of the bridged CO species on the Pd/Rh solid is slightly lower than that determined on Pd/La<sub>2</sub>O<sub>3</sub>/CeO<sub>2</sub>/Al<sub>2</sub>O<sub>3</sub>. For instance, at  $\theta = 0.9$ , the heats of adsorption of the B species are 105 and 120 kJ/mol on the bimetallic and monometallic solid respectively. This indicates either an interaction between Pd and Rh or the formation of bridged CO species on Pd–Rh sites.

### ACKNOWLEDGMENTS

The authors acknowledge the Faurecia Co., BP 17, Bois sur prés, 25550, Bavans, France, which supported this work.

### REFERENCES

1. Chafik, T., Dulaurent, O., Gass, J. L., and Bianchi, D., *J. Catal.* **179**, 503 (1998).
2. Dulaurent, O., Chandès, K., Bouly, C., and Bianchi, D., *J. Catal.* **188**, 237 (1999).
3. Dulaurent, O., Chandès, K., Bouly, C., and Bianchi, D., *J. Catal.* **192**, 273 (2000).
4. Bianchi, D., Bouly, C., Gass, J. L., and Maret, D., *Bull. Soc. Chim. Fr.* **128**, 130 (1991).
5. Bianchi, D., Gass, J. L., Bouly, C., and Maret, D., S.A.E. paper no. 910839, 1992.
6. Armor, J. N., *Appl. Catal. B. Environ.* **1**, 221 (1992).
7. Engler, B. H., Lindner, D., Lox, E. S., Schafer-Sindlinger, A., and Ostgathe, K., *Stud. Surf. Sci. Catal.* **96**, 441 (1995).
8. Anderson, J. A., and Rochester, C. H., *J. Chem. Soc., Faraday Trans.* **87**, 1479 (1991).
9. Solymosi, F., and Pasztor, M., *J. Catal.* **104**, 312 (1987).
10. Solymosi, F., Rasko, J., and Bontovics, J., *Catal. Lett.* **19**, 257 (1993).
11. Van Slooten, R. F., and Nieuwenhuys, B. E., *J. Catal.* **122**, 429 (1990).
12. Anderson, J. A., *J. Catal.* **142**, 153 (1993).
13. Yates, J. T., Duncan, T. M., Worley, S. D., and Vaughan, R. W., *J. Chem. Phys.* **70**, 1219 (1979).
14. Efstathiou, A. M., Chafik, T., Bianchi, D., and Bennett, C. O., *J. Catal.* **148**, 224 (1994).

15. Buchanan, D. A., Hernandez, M. E., Solymosi, F., and White, J. M., *J. Catal.* **125**, 456 (1990).
16. Lavalley, J. C., Saussey, J., Lamotte, J., Breault, R., Hindermann, J. P., and Kinnemann, A., *J. Phys. Chem.* **94**, 5941 (1990).
17. Rasband, P. B., and Hecker, W. C., *J. Catal.* **139**, 551 (1993).
18. Hicks, R. F., Yen, Q. J., and Bell, A. T., *J. Catal.* **89**, 498 (1984).
19. Srinivas, G., and Chuang, S. S. C., *J. Catal.* **144**, 131 (1993).
20. Bourane, A., Dulaurent, O., and Bianchi, D., *J. Catal.* (submitted).
21. Dubois, L. H., and Somorjai, G. A., *Surf. Sci.* **91**, 514 (1980).
22. Dubois, L. H., Hansma, P. K., and Somorjai, G. A., *J. Catal.* **65**, 318 (1980).
23. Dubois, L. H., Hansma, P. K., and Somorjai, G. A., *Appl. Surf. Sci.* **6**, 185 (1980).
24. Delouise, L. A., White, E. J., and Winograd, N., *Surf. Sci.* **147**, 252 (1984).
25. Beutler, A., Lundgren, E., Nyholm, R., Andersen, J. N., Setlik, B., and Heskett, D., *Surf. Sci.* **371**, 381 (1997).
26. Chang, C. M., Aris, R., and Weinberg, W. H., *Appl. Surf. Sci.* **1**, 360 (1978).
27. Castner, D. G., Sexton, B. A., and Somorjai, G. A., *Surf. Sci.* **71**, 519 (1978).
28. Thiel, P. A., Williams, E. D., Yates, J. T., and Weinberg, W. H., *Surf. Sci.* **84**, 54 (1979).
29. Belton, D. N., and Schmieg, S. J., *Surf. Sci.* **202**, 238 (1988).
30. Castner, D. G., and Somorjai, G. A., *Surf. Sci.* **83**, 60 (1979).
31. Batteas, J. D., Gardin, D. E., Van Hove, M. A., and Somorjai, G. A., *Surf. Sci.* **297**, 11 (1993).
32. Bowker, M., Guo, Q., and Joyner, R., *Surf. Sci.* **253**, 33 (1991).
33. Baraldi, A., Dhanak, V. R., Comelli, G., Prince, K. C., and Rosei, R., *Surf. Sci.* **293**, 246 (1993).
34. Nehasil, V., Stara, I., and Matolin, V., *Surf. Sci.* **331**, 105 (1995).
35. Campbell, C. T., and White, J. M., *J. Catal.* **54**, 289 (1978).
36. Somorjai, G. A., "Chemistry in Two Dimensions." Cornell Univ. Press, Ithaca, NY, 1981.
37. Brennan, D., and Hayes, F. H., *Philos. Trans. R. Soc. (London) A* **258**, 347 (1965).
38. Dhanak, V. R., Baraldi, A., Comelli, G., Paolucci, G., Kiskinova, M., and Rosei, R., *Surf. Sci.* **295**, 287 (1993).
39. Rebholz, M., Prins, R., and Krusz, N., *Surf. Sci.* **259**, L797 (1991).
40. Savargaonkar, N., Khnanra, B. B., Pruski, M., and King, T. S., *J. Catal.* **162**, 277 (1996).
41. Chuang, S. S. C., and Tan, C. D., *Catal. Today* **35**, 369 (1997).